INSTITUTE OF PHYSICS PUBLISHING JOURNAL OF PHYSICS: CONDENSED MATTER

J. Phys.: Condens. Matter **17** (2005) 3305–3315 doi:10.1088/0953-8984/17/21/023

Propagation of magnetic and superconducting order in Gd/La superlattices

P P Deen[1,5], J P Goff[1], R C C Ward[2], M R Wells[2], S Langridge[3], R Dalgliesh[3], S Foster[3] and G J McIntyre[4]

[1] Department of Physics, Oliver Lodge Laboratory, University of Liverpool, Liverpool, UK
[2] Oxford Physics, Clarendon Laboratory, Oxford OX1 3PU, UK
[3] The ISIS Facility, Rutherford Appleton Laboratory, Didcot OX11 0RA, UK
[4] Institut Laue Langevin, 156X, 38042 Grenoble Cedex 9, France

E-mail: deen@esrf.fr

Received 10 November 2004, in final form 12 April 2005
Published 13 May 2005
Online at stacks.iop.org/JPhysCM/17/3305

Abstract

Single-crystal Gd/La superlattices have been grown by molecular beam epitaxy. The magnetic ordering has been determined using neutron scattering and the superconducting transitions have been identified using SQUID magnetometry. The Gd layers order ferromagnetically below $T \sim 280$ K and the interlayer coupling across the La layers is antiferromagnetic. Surprisingly, when cooled in zero field below $T \sim 5$ K the Gd/La superlattices exhibit 3D superconductivity, even when the thickness of the La blocks is only 13 atomic planes. The transition from the normal to the superconducting phase does not affect the magnetic structure. In contrast, field cooling results in ferromagnetic coupling of the Gd blocks and, under these conditions, the superconducting transition is suppressed.

(Some figures in this article are in colour only in the electronic version)

1. Introduction

Previous studies of the interplay between the antagonistic phenomena of superconductivity and ferromagnetism using artificial nanostructures, comprising alternating superconducting (SC) and ferromagnetic (FM) layers, have produced fascinating results [1]. For example, as the superlattice composition is varied in Fe/V superlattices there is a crossover from 2D to 3D superconductivity, and the results imply the coexistence of superconductivity and ferromagnetism in the Fe layers [2]. The results also suggested a non-monotonic dependence of the superconducting transition temperature T_c on the thickness of the ferromagnetic layers.

[5] Author to whom any correspondence should be addressed. Present address: European Synchrotron Radiation Facility, BP 220, 38043 Grenoble Cedex 9, France.

Table 1. Structural parameters for Gd/La superlattices using the model of Jehan *et al* [13]. N gives the nominal number of bilayer repeats. Interface roughness/interdiffusion is denoted by λ. The average layer thickness of element x in a bilayer is given by D_x and d_x gives the average interplanar spacing of element x.

Sample	N	D_{Gd} ±3.11 (Å)	D_{La} ±2.95 (Å)	d_{Gd} ±0.005 (Å)	d_{La} ±0.005 (Å)	λ ±3.02 (Å)	Mosaic ±0.02 (deg)
I	60	80.86	38.22	2.916	3.023	9.1	1.41
II	60	90.19	49.98	2.937	3.101	12.1	1.67

This provoked intense theoretical interest in the proximity effect between the superconductor and the ferromagnet [3]. Oscillation of T_c was predicted [4] and subsequently measured using Gd/Nb superlattices [5]. This result implies a phase difference between the superconducting order parameter in neighbouring Nb layers. Calculations indicate that the superconducting characteristics depend strongly on the mutual orientation of the ferromagnetic layers, and a novel superconducting spin valve device was proposed [6]. A proof-of-principle experiment on a CuNi/Nb/CuNi trilayer in which one ferromagnetic layer is exchange biased and the other is free to respond to an applied field has shown a decrease of several millikelvins in T_c when the CuNi layers change their magnetization directions from parallel to antiparallel [7].

The discovery of the propagation of magnetic ordering through non-magnetic spacer layers in rare-earth superlattices has opened a new window on the nature of exchange coupling in the metallic state [8, 9]. For FM/non-magnetic Gd/Y superlattices the interlayer exchange between successive Gd blocks was found to oscillate as a function of Y thickness. This was one of the first magnetic phenomena to be shown to depend on the artificial periodicity of the superlattice [10]. In the case of FM/SC superlattices, pair breaking suppresses the superconductivity below a critical thickness of the superconducting layer [11], and in all previous studies of the proximity effect in superlattices the thickness of the superconducting layer has been too great to allow propagation of the magnetic order. In this paper we describe studies of Gd/La superlattices with superconducting La layers that are thin enough to allow propagation of the magnetic order, so that it is possible to correlate for the first time in a superlattice the superconducting behaviour with details of the magnetic structures.

2. Sample characterization

Single-crystal Gd/La superlattices have been grown using molecular beam epitaxy at the Clarendon Laboratory. The samples were grown on a Al_2O_3 [1 1 0] substrate with a 90 Å Nb [1 1 0] buffer and 1000 Å Y [0 0 1] seed layer, and they were capped with 300 Å of Y to prevent reaction with the atmosphere. Such a multi-component epitaxial system produces rare-earth superlattices of high structural quality and with the growth direction along [0 0 1]. Light rare-earth superlattices deteriorate over a period of a few months [12] and, as a consequence, two samples were required to complete the measurements. The crystal structures were determined using x-ray diffraction at the University of Liverpool. Figure 1(a) shows the x-ray intensity as a function of wavevector transfer **Q** along the [0 0 L] direction of the hexagonal close-packed (hcp) structure. The solid line shows the fit of the model by Jehan *et al* [13] for the structure of the average bilayer. The results are listed in table 1. The parameters in the model are the average layer thickness of each element, D_{Gd} and D_{La}, their interplanar spacings, d_{Gd} and d_{La}, and the extent of interdiffusion and roughness at the interface λ. Samples I and II have slightly different structural parameters, but essentially the same magnetic properties.

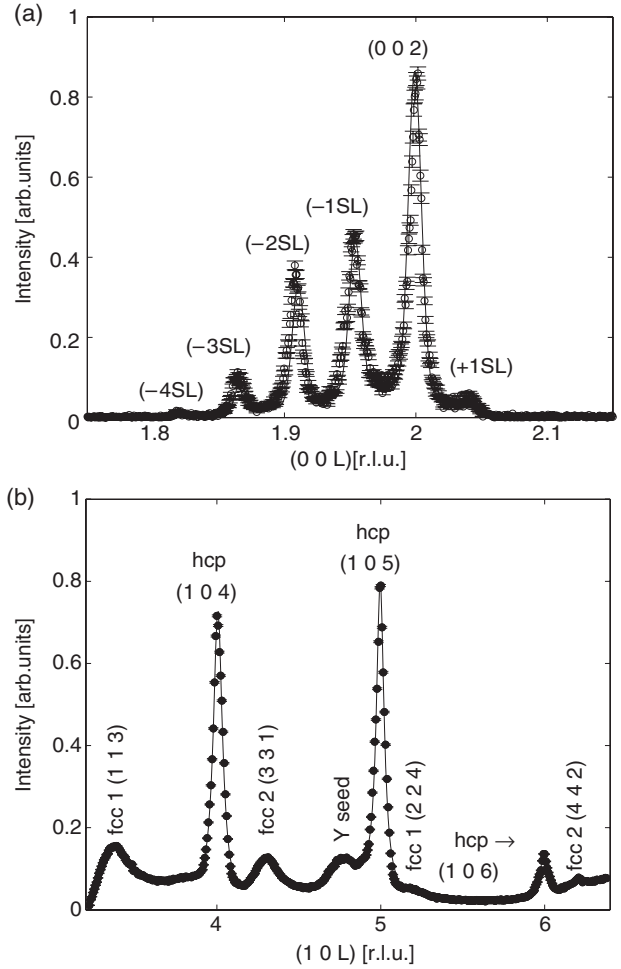

Figure 1. (a) Scan along the [0 0 L] direction for sample II. The solid line is a fit to the experimental data with parameters given in table 1. (b) Scan along the [1 0 L] direction with Gd hcp and La fcc peaks indexed.

Scans of wavevector transfer along $\mathbf{Q} = [1\ 0\ L]$ are sensitive to the stacking sequence of close-packed planes along the growth direction. Scans of this type are therefore used to determine the crystal structure within individual blocks. Figure 1(b) is the observed x-ray intensity along the hcp [1 0 L] direction for sample II. The peaks in figure 1(b) can be indexed using the Gd hcp lattice with additional peaks due to two domains of the La face-centred cubic (fcc) structure. The correlation lengths, obtained via the widths of the peaks in figure 1(b), correspond to coherence of these stacking sequences confined to the individual hcp and fcc blocks of Gd and La respectively. Note that, in contrast, the scattering along $\mathbf{Q} = [0\ 0\ L]$ is insensitive to the stacking sequence and the width of the peaks in figure 1(a) indicates that the positions of the close-packed planes are coherent over several bilayers.

3. Magnetization measurements

Magnetization measurements were performed using a Quantum Design SQUID magnetometer at the University of Liverpool with a temperature range 1.8–300 K. In addition to magnetization

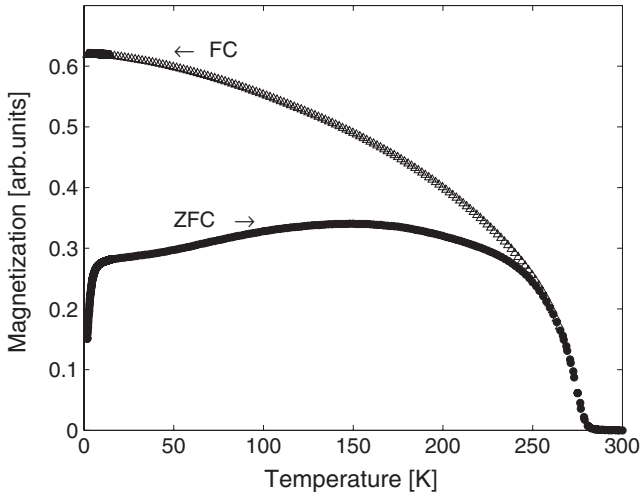

Figure 2. The ZFC and FC magnetization curves for sample I with $H = 50$ Oe applied in the sample plane.

measurements from the superlattices, control measurements were also performed on La and Nb thin films to characterize the non-superlattice component and the behaviour of La in a thin film sample.

Typical magnetization measurements for field cooling (FC) and zero-field cooling (ZFC) of the superlattices are shown in figure 2. A magnetic transition occurs for both the FC and ZFC cases at $T \sim 280$ K, a slight reduction from the Gd bulk transition temperature $T_c = 293$ K. Figure 2 clearly shows that FC and ZFC give rise to different magnetic ordering. For the ZFC curves there is a diamagnetic response below $T \sim 5$ K indicating the onset of superconductivity. The magnitude of the diamagnetic response indicates a superconducting volume fraction of a few per cent. The magnetization lineshape in the ZFC phase increases above the superconducting transition, indicating antiferromagnetic correlations. In contrast, cooling in a small field, 50 Oe, suppresses the superconductivity to below $T \sim 1.8$ K. In this case the magnetization lineshape is reminiscent of ferromagnetic order. It is surprising that the superconducting transition temperature T_c is close to the value for bulk fcc La since the blocks are only 38.22 Å, 13 monolayers, thick.

It can be correctly pointed out that resistivity measurements would complement the magnetization measurements in the verification of superconducting order. Unfortunately this is not possible for these systems. The superlattices require a Nb buffer to minimize the reaction between the substrate and the superlattice. Although the Nb diamagnetic signal is negligible with respect to the La signal, it would nevertheless act as an electrical short circuit when Nb becomes superconducting.

The dimensionality of the superconducting wavefunction may be determined using the Ginzburg–Landau equations modified to incorporate the anisotropy found in superlattices [14]. The critical magnetic fields applied parallel and perpendicular to the plane are given by

$$\mathbf{H}_{c\parallel} \propto \frac{1}{\xi_x \xi_z}, \qquad \mathbf{H}_{c\perp} \propto \frac{1}{\xi_x^2}, \tag{1}$$

where $\xi_{x,z}$ are the coherence lengths in (x) and out (z) of the plane of the superlattice, and these are related to the transition temperatures by $\xi_{x,z} \propto [1 - T/T_c]^{-1/2}$. T_c and T are superconducting transition temperatures in zero and applied field respectively. In a thin film

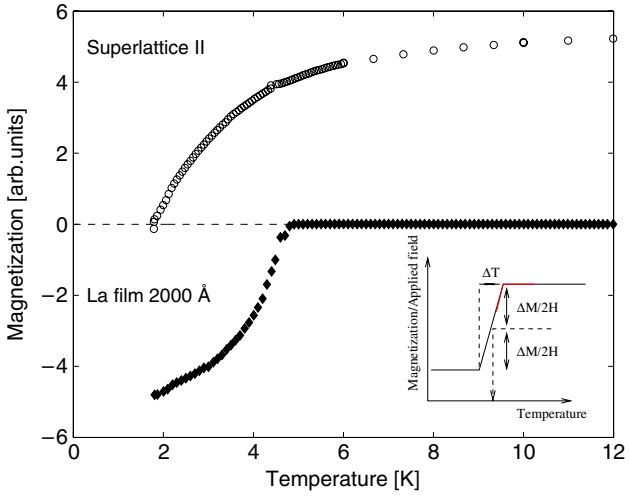

Figure 3. Typical magnetization curves for 2000 Å La thin film and a Gd/La superlattice obtained in an applied field of 50 Oe ∥ to the sample plane. The magnetization of the superlattice has been normalized with respect to the graph to facilitate comparison.

the out-of-plane coherence length is limited by the thickness of the film, d, for distances $\xi_z \sim d$. It is, therefore, possible to distinguish between 2D and 3D superconductivity via the temperature dependence of the parallel critical field

$$\mathbf{H}_{\parallel} \propto \begin{cases} \sqrt{\left(1 - \dfrac{T}{T_c}\right)} & \textbf{2D}, \\ \left(1 - \dfrac{T}{T_c}\right) & \textbf{3D}. \end{cases} \tag{2}$$

Figure 3 shows typical magnetization lineshapes for the superlattices and the La thin film. The 2000 Å La thin film reveals a sudden diamagnetic downturn around 5 K. There is negligible magnetic response above this transition. In contrast, the Gd blocks in the superlattice provide a magnetic state within the superlattice before the superconducting order occurs and so a net magnetic moment at the transition temperature is observed. Furthermore, the superlattice experiences a broad transition that has not been completed by the lowest temperature probed, 1.8 K. Determination of the transition temperature is therefore difficult. The common method employed to determine the superconducting transition temperature is shown in the inset of figure 3. The transition temperature is defined as the point of inflexion on the $M(T)$ dependence between zero magnetization and the constant minimum. This is clearly not possible for these systems. Instead a relative transition temperature can be determined if two assumptions are made. First, it is assumed that for each sample the transition width, ΔT, remains constant as the applied field is varied. Second, the maximum magnetic susceptibility of the system must also be a constant as a function of applied field. These assumption are valid since the transition width is representative of the crystalline disorder and the saturation susceptibility is not dependent on the magnitude of the applied field. The relative transition temperature can now be defined as the temperature where the susceptibility has diminished by a fraction of the maximum susceptibility.

The dependence of the superconducting transition temperature on applied field is presented in figure 4. A linear relationship is obtained between $H_{\perp}$ and $(1 - T/T_c)$, as expected from

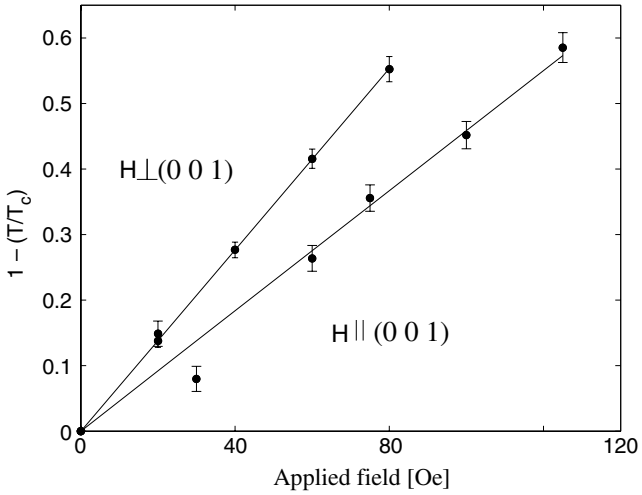

Figure 4. The application of a field both in and out of the plane results in a linear relationship, $H \propto (1 - T/T_c)$, a signature of three-dimensional superconductivity in anisotropic structures.

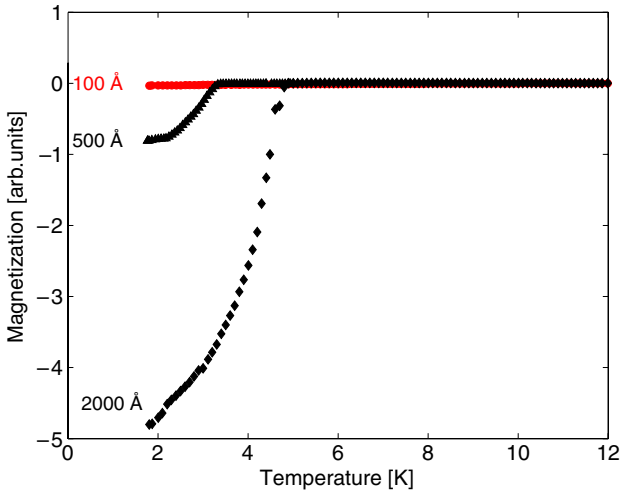

Figure 5. Temperature dependence of the magnetic susceptibility of La thin films with varying thicknesses.

equation (1). The dependence between the applied field and $(1 - T/T_c)$ for the field applied parallel to the plane is also linear. This directly demonstrates the 3D superconducting behaviour and, therefore, tunnelling of the superconducting order parameter through the ferromagnetic Gd blocks.

In control measurements we have determined the effect of decreasing thickness on T_c directly for La thin films. We find that the superconducting behaviour of a 2000 Å thick La film is similar to the superlattices with $T_c \sim 5$ K, a 500 Å film has a reduced $T_c \sim 3.5$ K, and the diamagnetic response is negligible for a film with 100 Å La. Figure 5 clearly demonstrates this behaviour and supports the result that the superconducting order parameter tunnels through the ferromagnetic Gd blocks. Nevertheless, it is well known that T_c rises sharply with pressure

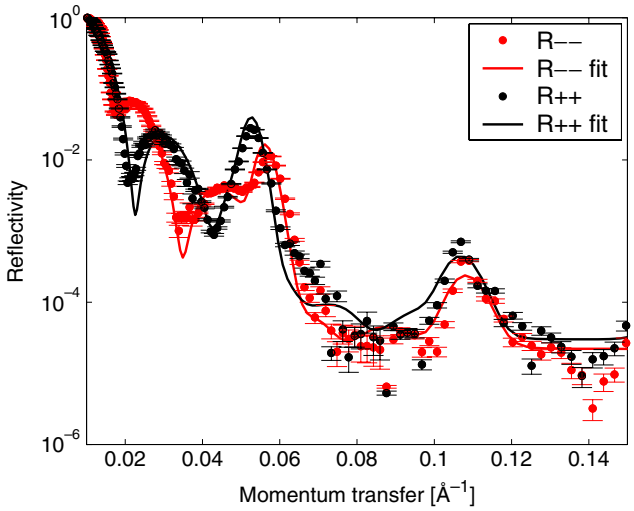

Figure 6. PNR for sample I at $T \sim 3$ K after FC; the lines are a fit for ferromagnetic order of the Gd blocks with structural parameters obtained from x-ray diffraction.

for La [15]. It is therefore possible that the chemical pressure induced by the epitaxial strain in the thin films and superlattices could enhance T_c. However, we note that the in-plane lattice parameters for all of the La thin films and Gd/La superlattices are similar. The thin film measurements therefore constitute a good baseline for the superlattice studies and make the observation of superconductivity in superlattices with 39 Å La blocks all the more remarkable.

Further control measurements on a Al_2O_3 substrate with a 90 Å Nb buffer and 1000 Å Y film revealed a negligible temperature dependence of the magnetization. This confirms that the signal in figure 2 is dominated by the Gd/La superlattice.

4. Neutron scattering

The complementary techniques of polarized neutron reflectivity (PNR) and neutron diffraction were used to determine the magnetic structures in the ZFC and FC phases. Reflectivity and diffraction scattering profiles were measured as a function of momentum transfer $\mathbf{Q}$, and provide information on the moment directions and the magnetization profile through the sample.

4.1. Polarized neutron reflectivity

PNR measurements were performed using the CRISP reflectometer at the ISIS Facility with both spin $1/2$ and spin $-1/2$ incident neutrons. The non-spin flip reflectivities were measured with a 99% efficient supermirror discarding unwanted eigenstates. The cross sections R++ and R$--$ were measured. Since neutrons interact with the magnetic state of the system the non-spin flip reflectivities measured by PNR, R++ and R$--$, differ for a magnetically ordered system.

PNR was performed in both the FC and ZFC states. A small magnetic field, $H = 20$ Oe, was applied in the plane before cooling to achieve the FC state and after cooling for the ZFC state. Figure 6 shows the non-spin flip reflectivities R++ and R$--$ in the FC phase at $T \sim 3$ K for sample I. The solid lines show fits to the data for a model corresponding to ferromagnetic

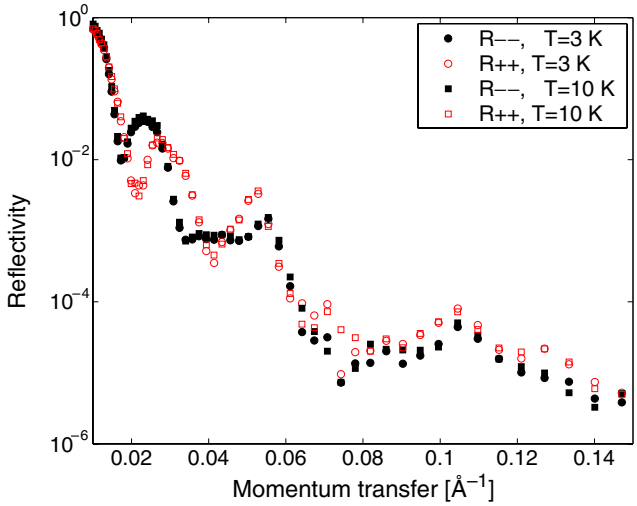

Figure 7. Comparison of the superconducting phase at $T \sim 3$ K and the normal phase at $T \sim 10$ K. The difference between R++ and R−− shows the existence of magnetic order. There is no change in the profiles obtained for the superconducting and normal phases.

aligned Gd blocks with $\mu = 5.7 \pm 0.2\ \mu_B$/atom, a reduced value from the saturated ionic moment in the bulk, 7 μ_B. Since neutrons are sensitive to the magnetization perpendicular to **Q** this corresponds to the in-plane component of the moment. This moment is consistent with our SQUID measurements and corresponds to a polarized neutron study of Gd/Y superlattices by Majkrzak *et al* [8]. They determined a value of 5.4 μ_B per Gd atom for a Gd/Y superlattice with 10 atomic planes of Gd per bilayer repeat.

Figure 7 shows the reflectivity profiles below and above T_c at 3 and 10 K in the ZFC phase. The difference between R++ and R−− indicates a magnetically ordered system, the structure of which cannot be modelled with simple long-range antiferromagnetic (AF) or ferromagnetic structures. The interesting feature of figure 7 is the exact superpositition of the reflectivity profiles, R++ and R−−, obtained above and below the superconducting transition temperature. Hence magnetic order of the Gd blocks has not been affected by the superconducting state and PNR is insensitive to the flux exclusion in the La blocks. Hence, the onset of superconductivity and the creation of an energy gap, required for BCS superconductivity, does not affect the magnetic coupling between the Gd blocks.

4.2. Neutron diffraction

The magnetic structure of the ZFC phase was determined by neutron diffraction using beamline D10 at the ILL. Figure 8(a) shows the neutron intensity in the vicinity of the hcp (0 0 2) Bragg peak in the paramagnetic phase. The solid line depicts the scattering calculated using the structural parameters determined separately by x-ray diffraction. Figure 8(b) displays the extra scattering observed as the temperature is lowered to $T \sim 1.5$ K. Scattering along the hcp [0 0 L] direction is only sensitive to the position of the atoms along the c-axis. Neutron diffraction with momentum transfer along the hcp [0 0 L] direction is therefore a probe of the in-plane magnetic moments in the Gd blocks as a function of depth through the superlattice. The magnetic scattering observed in figure 8(b) occurs between the positions of the structural peaks of figure 8(a) and is therefore due to antiferromagnetic correlations. The subtraction

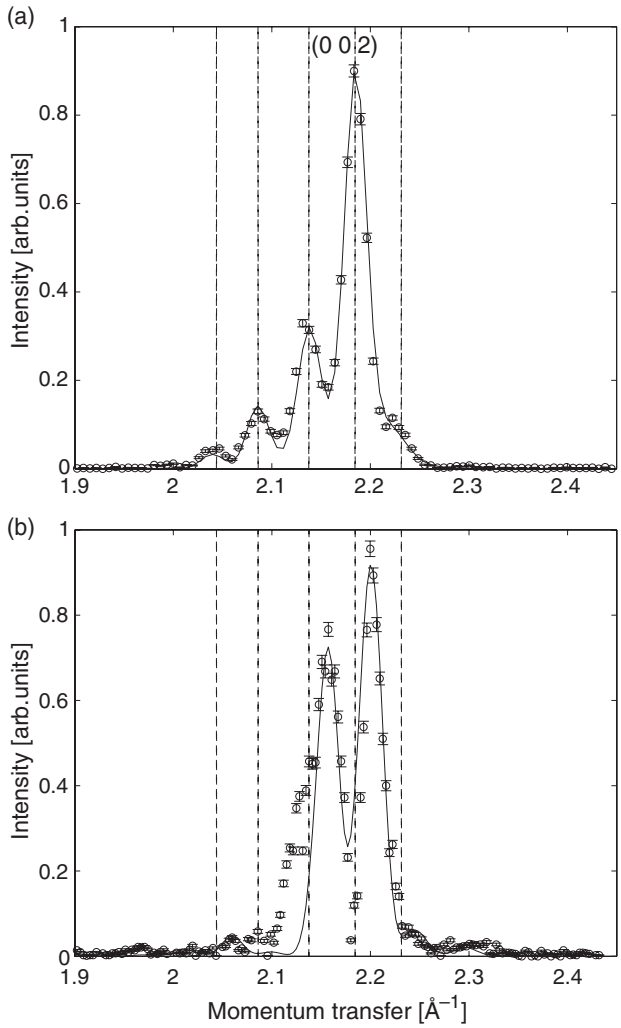

Figure 8. (a) Neutron diffraction from sample II near the hcp (0 0 2) peak at $T \sim 300$ K in the paramagnetic phase. (b) The additional intensity observed at $T \sim 1.5$ K as a result of magnetic order. The sold lines show the calculated scattering using (a) the structural parameters of the superlattice and (b) a model of antiferromagnetic (AF) short-range order coherent across two to three bilayer repeats. The dashed lines show the positions of the structural superlattice reflections.

of structural scattering is imperfect due to the change in lattice parameters between $T \sim 300$ and 1.5 K. However, short-range antiferromagnetic correlations between the Gd blocks with an average coherence across two to three bilayers is able to provide qualitative agreement with the data. The solid line in figure 8(b) represents such short-range antiferromagnetic order.

Scattering along [1 0 L] is sensitive to the stacking sequence of the system and, as explained in section 2, will probe the correlations within individual blocks. Neutron diffraction along the hcp [1 0 L] direction probes the magnetic order within the Gd blocks. Figure 9 shows the neutron scattering along the hcp [1 0 L] direction in the ZFC phase. The structural hcp peaks obtained at 300 K are enhanced by magnetic scattering as the temperature is reduced to $T \sim 1.5$ K. Ferromagnetic order therefore exists within the Gd blocks.

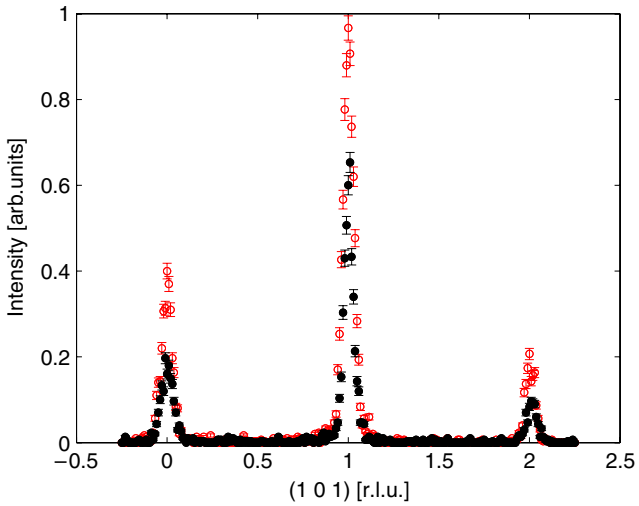

Figure 9. Neutron diffraction from sample II near the hcp (1 0 1) peak at $T \sim 300$ K, ∘, and at $T \sim 2$ K, ∘. Magnetic order within the blocks is ferromagnetic.

Neutron scattering and SQUID magnetometry have enabled the complete determination of the magnetic structures in the FC and ZFC phases. In the ZFC phase short-range antiferromagnetic correlations exist between ferromagnetic Gd blocks, thus giving rise to a net magnetic moment in the ordered state at the onset of 3D superconductivity. In contrast, in the FC phase ferromagnetic coupling of the Gd blocks suppresses the superconducting transition.

5. Conclusions

The effect of the magnetic ordering on the superconductivity in Gd/La superlattices is reminiscent of the behaviour of erbium rhodium boride, where the formation of domain-like structures below $T \sim 1.2$ K allows the coexistence of ferromagnetism and superconductivity, whereas the formation of a single-domain ferromagnet below $T \sim 0.71$ K completely destroys the superconductivity [16]. The ZFC phase of Gd/La and the domain-like structure in $ErRh_4B_4$ have periodicities that are much greater than the atomic distances, but smaller than the size of the Cooper pairs, and the superconductivity survives because the magnetic structure looks like an antiferromagnet from the large-scale viewpoint of superconductivity [17]. The ordering temperatures show that the energy scale of the magnetism is much greater than that of the superconductivity. Thus magnetism is the more robust phenomenon and the onset of superconductivity in Gd/La does not affect the magnetic ordering.

These rare-earth superlattices exhibit some of the properties desirable in a superconducting spin-valve device. First, the change in the superconductivity is much more pronounced than the rather subtle changes observed in the transition-metal systems so far. Second, antiferromagnetic alignment of the ferromagnetic blocks is required in the absence of a field. These are the first superconducting superlattices to spontaneously order in this manner.

In summary, we have observed 3D magnetism and superconductivity in Gd/La superlattices and this sheds new light on the interaction between these usually mutually exclusive phenomena.

Acknowledgment

We would like to acknowledge funding from EPSRC grant GR/R13845.

References

[1] Izyumov Y A, Proshin Y N and Khusainov M G 2002 *Phys.—Usp.* **45** 109
[2] Wong H K, Yang H Q, Hilliard J E and Ketterson J B 1985 *J. Appl. Phys.* **57** 3660
[3] Wong H K, Yin B Y, Yang H Q, Ketterson J B and Hilliard J E 1986 *J. Low Temp. Phys.* **63** 307
[4] Radović Z, Ledvij M, Dobrosavljević-Grujić L, Buzdin A I and Clem J R 1991 *Phys. Rev.* B **44** 759
[5] Jiang J S, Davidović D, Reich D H and Chien C L 1995 *Phys. Rev. Lett.* **74** 314
[6] Tagirov L R 1999 *Phys. Rev. Lett.* **83** 2058
[7] Gu J Y, You C Y, Jiang J S, Pearson J, Bazaliy Ya B and Bader S D 2002 *Phys. Rev. Lett.* **89** 267001
[8] Majkrzak C F, Cable J W, Kwo J, Hong M, McWhan D B, Yafet Y, Waszczak J V and Vettier C 1986 *Phys. Rev. Lett.* **56** 2700
[9] Salamon M B, Sinha S, Rhyne J J, Cunningham J E, Erwin R W, Borchers J and Flynn C P 1986 *Phys. Rev. Lett.* **56** 259
[10] Kwo J, Hong M, DiSalvo F J, Waszczak J V and Majkrzak C F 1987 *Phys. Rev.* B **35** 7295
[11] Strunk C, Surgers C, Paschen U and Lohneysen H v 1994 *Phys. Rev.* B **49** 4053
[12] Ward R C C, Wells M R, Bryn-Jacobsen C, Cowley R A, Goff J P, McMorrow D F and Simpson J A 1996 *Thin Solid Films* **275** 137
[13] Jehan D A, McMorrow D F, Cowley R A, Ward R C C, Wells M R, Hagmann N and Clausen K N 1993 *Phys. Rev.* B **48** 5594
[14] Tinkham M 1963 *Phys. Rev.* **129** 2413
[15] Probst C and Wittig J 1978 *Handbook of Physics and Chemistry of Rare Earths* No. 752 (Amsterdam: Elsevier)
[16] Sinha S K, Crabtree G W, Hinks D G and Mook H 1982 *Phys. Rev. Lett.* **48** 950
[17] Anderson P W and Suhl H 1959 *Phys. Rev.* **116** 898